Fatigue Fract. Engng Mater. Struct. Vol. 17, No. 5, pp. 551–561, 1994
Printed in Great Britain.

8756-758X/94 $6.00+0.00

ELEVATED TEMPERATURE FATIGUE CRACK GROWTH BEHAVIOR OF Ti-1100

B. K. PARIDA[1] and T. NICHOLAS[2]

[1]Structural Integrity Division, National Aeronautical Laboratory, Bangalore 560017, India
[2]WL/MLLN, Wright-Patterson Air Force Base, Ohio 45433–6533, U.S.A.

Received in final form 28 January 1994

Abstract—The fatigue crack growth behavior of Ti-1100 is analyzed at elevated temperatures to evaluate the effects of mechanical and environmental variables. Experiments conducted over a wide range of frequencies from 0.01 Hz to 200 Hz indicate a strong dependence of the growth rate upon cyclic loading frequency. Superposition of hold time at maximum and minimum loads over a baseline 1.0 Hz cyclic loading frequency produces an insignificant variation in crack growth rate, which may be attributed to the combined effects of enhanced environmental degradation, crack-tip blunting and increased asperity-induced closure level in this material. It is deduced that a hold time at maximum load results in an interaction of the environmental effects with a retardation effect due to crack tip blunting as a consequence of creep under maximum applied load, whereas for hold at minimum loads, extensive crack-branching and micro-cracking appear to enhance crack closure loads resulting in lower crack growth rates. A linear superposition model is employed to account for the complex interactions due to fatigue, creep and environmental degradation.

INTRODUCTION

Ti-1100 is a β-processed near-α titanium alloy recently developed by TIMET [1,2] to operate at a maximum temperature of 593°C (1100°F), which has an improvement of about 55°C in operating temperature over other conventional titanium alloys. Generally, β-processed near-α titanium alloys, such as Ti-6Al-4V, Ti-6242 S and IMI-829 exhibit superior fracture toughness and better fatigue resistance through improved energy absorption [3–5].

However, these alloys are prone to excessive creep and environmental damage at temperatures exceeding 538°C [6]. This has necessitated the development of newer alloys with higher temperature capability to be used in the compressor stages of next generation "hot" gas turbine engines and for replacement of nickel-base superalloys in present engines to effect weight savings. In order to get these materials into service, the damage tolerant design approach for any engine structural component requires that by prior analysis and testing it should be demonstrated that any pre-existing defects in the material will not grow to catastrophic proportions within a time span of half the inspection interval. This requires prediction of fatigue crack growth rate under service loading and temperature conditions typical for the component. Consideration has to be given to the time-dependent aspects due to both creep and environment. Based on an experimental study of Ti-1100 at elevated temperature, Ghonem *et al.* [3] have observed that the mechanisms governing environmentally assisted crack growth in this alloy are not completely understood. Parida and Nicholas [7] have noted that this material exhibits mixed cycle and time dependent crack growth in the higher frequency range, whereas at very low frequency environmental damage appears to be less significant compared to the cyclic damage contribution. Foerch *et al.* [8], while studying the environmental interactions at high temperature, have concluded that the effect of oxidation on the crack growth acceleration is rapid, is constant over the frequency range investi-

gated by them, and that crack growth rate is weakly dependent on cycle time. They also reported that creep effects are dominant at lower frequencies in both air and vacuum. What is not clearly understood is the fatigue-creep-environment interaction effects in Ti-1100, which is crucial for developing a fatigue crack growth prediction model at elevated temperature. In this study, the above interaction effects were critically examined through high temperature testing over a wide range of frequency, including superimposed hold times applied at maximum and minimum loads. A simple superposition model proposed earlier [9,10] to predict fatigue crack growth rate of Ti-24Al-11Nb, is employed here to predict the crack growth rate of Ti-1100 at 593°C.

EXPERIMENTAL PROCEDURE

The experiments conducted in this investigation involved the use of flat specimens made from Ti-1100 whose chemical composition in % weight is: 6.0 Al, 2.75 Sn, 4.0 Zr, 0.4 Mo, 0.45 Si, 0.07 O, 0.02 Fe, balance Ti. The material was beta-forged from 1093°C, hot rolled above the beta-transus to about 12 mm thick plates and stabilized at 593°C for 8 h. The resulting microstructure, shown in Fig. 1, consists essentially of transformed Widmanstatten basketweave formations with aligned colonies of α-platelets exhibiting no preferred orientation. The average size of prior β-grains was about 500–600 μm. The mechanical properties of this material at room temperature and at 593°C are as follows: Ultimate tensile stress: 980 MPa (674 MPa); 0.2% yield stress: 915 MPa (485 MPa); Young's modulus: 120 GPa (82 GPa); % elongation: 10–12 (10–12); % reduction in area: 21–30 (30); where the numbers in parentheses indicate corresponding values at 593°C.

For this investigation, flat single edge-notched tension, $SE(T)$ specimens of nominal dimensions 124 × 25 × 2.5 mm were machined along L–T orientation through electro-discharge machining. A sharp U-notch of nominal depth 2.5 mm and a notch width of 0.28 mm was machined at the mid-length of each specimen. The mid-section region of each specimen was electro-polished on both faces in order to permit easy monitoring of the optical crack length. For automated crack length measurement, a reversing D.C. potential drop technique was employed [10]. For this purpose, two pairs of electric potential (EP) leads were spot-welded to the notched edge of the specimen just above and below the U-notch with a nominal spacing of 5 mm. In order to provide a reference potential for normalization of the EP readings for use in Johnson's equation [11], another pair of EP leads was attached to the specimen length axis far away from the notch plane. The computed crack lengths were verified through optical crack length measurements from time to time. During the test, specimens were heated with two quartz lamps of 1 kW (3200 °K) capacity each on either

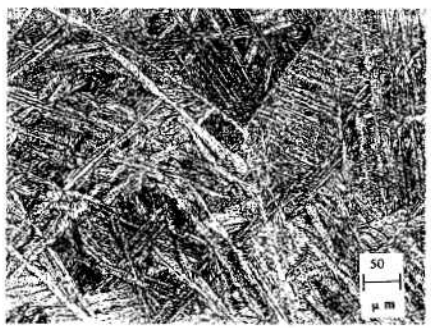

Fig. 1. Microstructure of Ti-1100 along L–T orientation.

side of the specimen and a Micricon controller was utilized to regulate the actual temperature in the crack plane of the specimen to within ±2°C of the preset temperature. Several thermocouples were fixed at different locations on both faces of the specimen to monitor temperature distribution and ensure its uniformity over the crack plane.

All tests in this investigation were carried out on a servo-controlled electro-hydraulic (major-minor) test system, incorporating an INSTRON model 1334 load frame with a large capacity (9.0 kN peak-to-peak) electro-dynamic shaker and an automated machine control as well as data acquisition system. The hydraulic actuator is used for application of cyclic loading in the low frequency range, typically from 0.01 Hz to 20 Hz, whereas for high frequency tests in the frequency range of 30 Hz to 550 Hz, the amplitude component is actuated by the electro-dynamic shaker while mean load is applied by the hydraulic actuator. During this investigation, fatigue crack growth rates were studied primarily at 593°C under lab-air conditions using pure cyclic loading with sinusoidal wave form. In order to evaluate the elevated temperature fatigue crack growth in Ti-1100, which has been shown to involve both environmental degradation through oxidation and crack-tip blunting due to creep, pure cyclic loading as well as superimposed hold time tests were carried out. For pure cyclic loading, frequencies of 0.01 Hz, 0.1 Hz, 1.0 Hz, 30 Hz, 100 Hz and 200 Hz were employed. Several additional tests were also conducted at an elevated temperature of 649°C in order to examine the behavior of this material at a temperature somewhat higher than the design temperature. In order to evaluate the influence of environmental effects on fatigue crack growth, hold-time tests were conducted with hold time durations of 10 s/cycle and 30 s/cycle at maximum as well as minimum loads superimposed over a 1.0 Hz baseline constant amplitude loading cycle. During the test, crack length was measured using reversing direct current potential drop (DCPD) method which was shown to be quite accurate through optical monitoring of crack length [10]. Fatigue crack growth rate, da/dN, was computed using a seven-point polynomial fit to the crack length and number of cycles data and was correlated with the stress intensity range, ΔK. Although an argument can be made regarding the applicability of LEFM based parameters to characterize time dependent crack growth, it has been shown by Larsen and Nicholas [12] that ΔK is suitable even where time dependent material behavior is encountered, as in nickel-base superalloys. More recently, Nicholas and Mall [13] and Parida and Nicholas [10] have shown ΔK to work quite well as a crack growth rate correlating parameter for a titanium aluminide alloy. From the test data, stress intensity range, ΔK, was computed using the standard formula for $SE(T)$ configuration. Data corresponding to a net-section stress level in excess of 90% of the material yield stress at 593°C were discarded. Unless otherwise specifically indicated, the stress ratio, $R = 0.1$ was used consistently throughout this investigation.

EXPERIMENTAL RESULTS

Figure 2 shows the frequency response of Ti-1100 at 593°C in terms of a plot of da/dN vs. ΔK. The variation of growth rate at any given ΔK shows a steady increase with decreasing frequency starting at 200 Hz, where two independent data sets are shown in order to demonstrate the reproducibility of test data. The increase in FCGR with decrease in frequency, f, almost levels off for $f \leq 1.0$ Hz. Figure 2 also shows a rather steep rise in fatigue crack growth rate corresponding to $\Delta K \approx 20$–25 MPa$\sqrt{\text{m}}$ at lower frequencies ($f \leq 1.0$ Hz).

SEM examination of fracture surfaces covering the entire range of crack growth reveals a change in fracture mode at different stress intensity range in this material. Figure 3 shows the SEM micrographs of fracture surfaces corresponding to different levels of stress intensity range at f = 1.0 Hz. At low stress intensity range, $\Delta K \leq 20$ MPa$\sqrt{\text{m}}$, the mode of fracture is quasi-cleavage

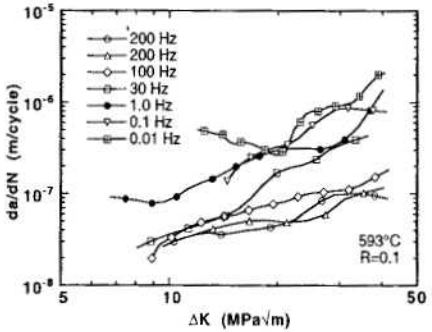

Fig. 2. Frequency response of Ti-1100 at 593°C.

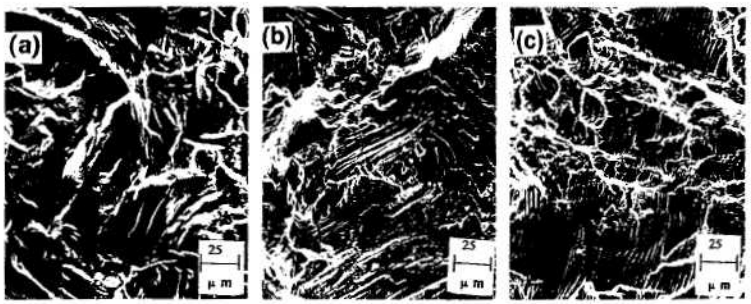

Fig. 3. SEM micrographs of fracture surfaces at 593°C at $f = 1.0$ Hz: (a) quasi-cleavage fracture mode at $\Delta K \leq 20$ MPa$\sqrt{m}$, (b) transition from quasi-cleavage to ductile tearing mode at $\Delta K \approx 20$–25 MPa$\sqrt{m}$, (c) striated crack growth at $\Delta K \approx 40$ MPa$\sqrt{m}$.

while in the high stress intensity range, $\Delta K \geq 40$ MPa$\sqrt{m}$, the fracture surface clearly indicates a ductile tear mode which is exhibited by striated crack growth. The transition from quasi-cleavage to a ductile tearing mode of crack growth is observed to occur in the range of $\Delta K \approx 20$–25 MPa$\sqrt{m}$.

The variation of fatigue crack growth rate with cycle time for a given stress intensity range of $\Delta K = 20$ MPa$\sqrt{m}$ is shown in Fig. 4 for the cyclic data. Here it can be clearly seen how growth rate tends to be independent of cycle time for times greater than approximately 1 s, that is, for frequencies below 1 Hz. Figure 5 shows growth rate curves which illustrate the effects of superimposed hold times at 593°C for holds at either maximum or minimum loads. Shown also, for reference purposes, are the cyclic growth rate data at frequencies of 100, 1, and 0.1 Hz. With the exception of the 100 Hz data, which clearly show the lowest growth rate, differences between the remaining data are almost indistinguishable. It is observed that crack growth rates for $f = 1.0$ Hz + 10 s and $f = 1.0$ Hz + 30 s with hold at either P_{max} or P_{min} exhibit almost identical values to each other as well as to data at either 1 Hz or 0.1 Hz. For the 10 s holds, the cycle time (11 s) is almost identical to that of the 0.1 Hz cycle. Based on the argument of increased growth rate per cycle due to greater environmental degradation with increased (exposure) cycle time, one would expect different growth rates for hold at maximum and minimum loads as well as for a decrease in frequency. It is clear that increasing the cycle time above approximately 1 s, whether by change in frequency or addition of hold time, has no net effect on growth rate. It is surmised that for hold

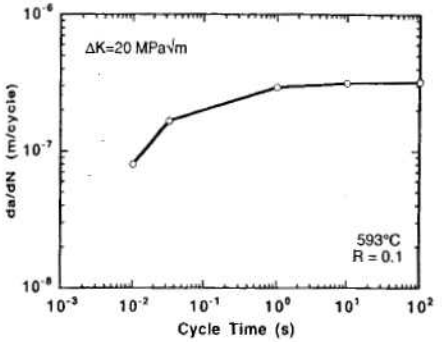

Fig. 4. Variation of fatigue crack growth rate with cycle time at $\Delta K = 20$ MPa$\sqrt{m}$.

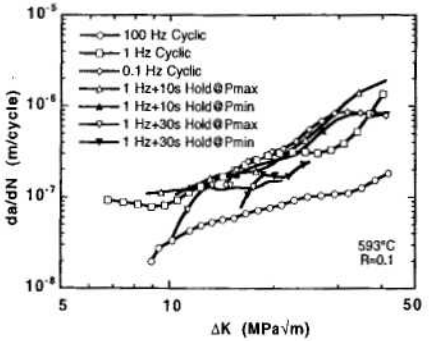

Fig. 5. Effects of superimposed hold time on $f = 1.0$ Hz baseline cycle at P_{max} and P_{min} on FCGR.

at maximum load or decrease in frequency, a possible reduction in crack-tip stress intensity occurs due to crack-tip-blunting induced by creep. This may be responsible for neutralizing the adverse effects of increased environmental degradation due to increased exposure time. For hold at minimum load ($R = 0.1$) however, creep effects causing blunting would be expected to be insignificant and not affect the growth rate. Since the growth rate remains at almost the same level as in the case of hold at maximum load or decrease in frequency, some other mechanism might be expected to be present. Therefore, a careful inspection of the crack-tip region on the specimen surface was made, before specimen failure, which revealed extensive crack branching and microcracking. Figure 6 shows optical micrographs of the specimen surface near the crack plane exhibiting crack deflection and a profusion of micro-cracks that accompany crack propagation at $f = 1.0$ Hz + 10 s hold at P_{min}. These features might be responsible for raising the crack closure level due to asperity induced closure, thereby reducing the crack growth rate. Walker *et al.* [14] and

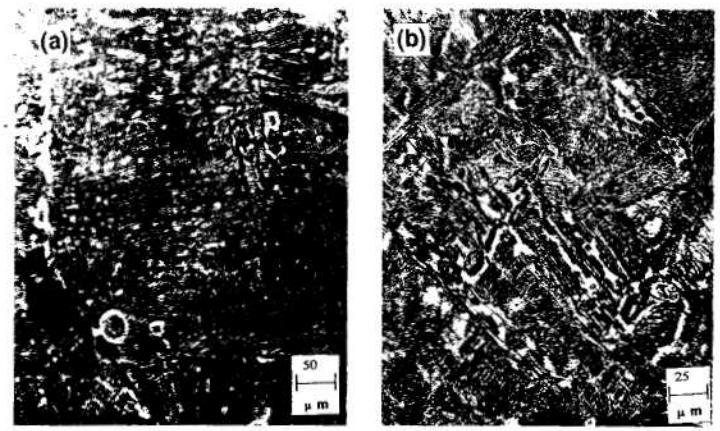

Fig. 6. Optical micrograph of crack tip region on specimen surface for $f = 1.0$ Hz + 10 sec hold at P_{min}: (a) crack deflection and extensive microcracking, (b) crack branching along with profusion of microcracks.

Halliday *et al.* [15] have reported the significance of crack closure on fatigue crack growth in near-α titanium alloys. Although no direct measurement of closure level was made in this investigation, based on the above circumstantial evidence including the optical micrographs as described above, it is believed that the relatively lower than expected crack growth rate in the case of superimposed hold times of 10 s and 30 s at minimum load is a consequence of increased level of asperity induced crack closure. Since no tests were conducted at different stress ratios other than 0.1, this hypothesis requires further investigation.

The time dependent crack growth or crack velocity, da/dt, versus cycle time is shown in Fig. 7, corresponding to $\Delta K = 20\ \text{MPa}\sqrt{\text{m}}$ for the entire frequency range under pure cyclic loading condition. The da/dt data presented here have been derived through interpolation fit of experimental data. Vacuum and laboratory air data [8] for $C(T)$ specimens at 593°C are also shown here for comparison purposes. Note that the three data sets represent three different specimen thicknesses as well as different geometries. It can be seen that the laboratory air data over a wide range of cycle times correlate very well irrespective of specimen geometry. It is only when approaching the highest cycle time, corresponding to $f = 0.01$ Hz, that the two data sets diverge slightly. The higher growth rate in the thicker (10 mm) $C(T)$ specimens might be due to the development of a smaller plastic or creep crack tip zone in plane strain than in the thinner (2.5 mm) $SE(T)$ specimens which are closer to plane stress. If creep affects the size of the inelastic zone near the crack tip, longer cycle times would provide more time for this zone to develop because of the slower crack velocity. Following the observations of Foerch *et al.* [8], it is postulated that creep effects in this material are dominant at lower frequencies, thus the growth rate is slower for thinner (plane stress) specimens with larger crack-tip plasticity compared to thicker (plane strain) specimens.

Figure 7 also shows a comparison of crack growth velocity (da/dt) data obtained in lab air against those obtained in vacuum on the same heat of material. The two curves are seen to be parallel and separated by approximately a factor of more than two. At shorter cycle times corresponding to high frequency, the environmental effects may be considered to be negligible, because of very little exposure time in a cycle. The crack velocity is highest at the high frequencies. Although no data were available for tests in vacuum at very high frequencies, an extrapolation of the straight line vacuum curve can be made. Consequently, the lab-air and projected vacuum data for lower cycle time appear to coincide. This observation implies that for cyclic loading, environmental effects in air are essentially absent at frequencies around 100–200 Hz and only become

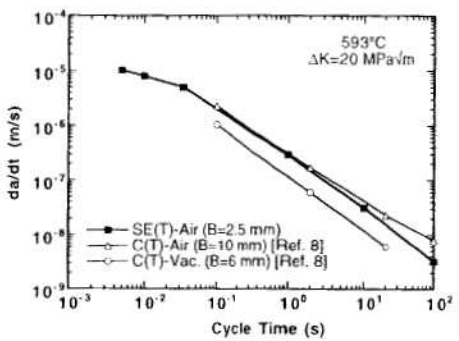

Fig. 7. Variation of time rate of crack growth with cycle time at 593°C, $\Delta K = 20\ \text{MPa}\sqrt{\text{m}}$.

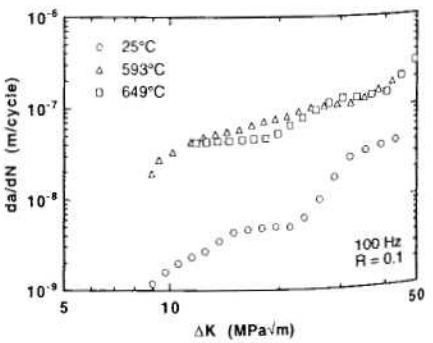

Fig. 8. Effects of temperature on fatigue crack growth rate in Ti-1100.

significant at frequencies below around 10 Hz or 0.1 s cycle time. It may further be seen from Fig. 4 and Fig. 7 that corresponding to higher range of frequencies (lower cycle times), fatigue crack growth rate strongly depends on cycle time in this material.

To explore the behavior of Ti-1100 at a higher temperature, two crack growth tests were conducted at 593°C and 649°C at a frequency of 100 Hz. These data are plotted in Fig. 8 which shows the effects of temperature on fatigue crack growth at 100 Hz and $R = 0.1$. It is seen that the growth rates at two elevated temperatures are higher than that at room temperature over the entire stress intensity range. However, there appears to be little difference in crack growth rates between 593°C and 649°C. The difference between the room temperature and the elevated temperature growth rates appears to lessen at the very high stress intensity range.

SEM micrographs of the fracture surface at 649°C, shown in Fig. 9, reveal two distinctly different modes of fracture dominating over the stress intensity range. Striated crack growth through ductile tearing, Fig. 9(a), occurs over the low to intermediate range of ΔK. This mode was observed at intermediate to high ΔK at 593°C. At high ΔK at 649°C, an intergranular fracture mode is observed (Fig. 9(b)). This is the only condition where this mode of failure is observed in this material. It should be noted that these comparisons and observations are confined to data and observations at a frequency of 100 Hz and $R = 0.1$. Considering the complex time-dependent behavior of this alloy, it would be unreliable to extrapolate the conclusions about the similarity of growth rates at 593°C and 649°C to other frequencies or stress ratios or other conditions involving hold times.

FATIGUE–CREEP–ENVIRONMENT INTERACTION MODEL

In order to help explain the complex interaction effects of fatigue, creep and environment on the fatigue crack growth rate of Ti-1100, a linear superposition model is adapted. This form of model was proposed earlier and used successfully [9,10] to characterize the high temperature growth rate behavior of a titanium aluminide, Ti-24Al-11Nb, which exhibited fatigue, creep blunting, and environmental effects at 649°C. Van Stone, [16] after an extensive analysis of an interpolation model and a superposition model in conjunction with experimental data for a nickel-base superalloy, concluded that the superposition model could correlate the experimental data reasonably well. In a linear superposition model, fatigue crack growth rate at any given stress intensity range may be represented as an algebraic sum of a cycle-dependent crack growth term

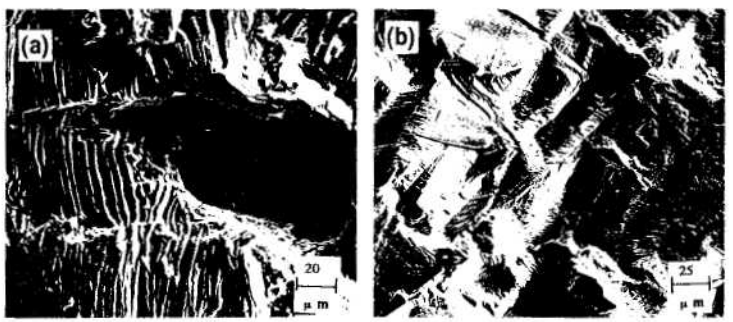

Fig. 9. SEM micrographs of fracture surfaces at 649°C: (a) striated crack growth through ductile tearing mode, (b) inter-granular fracture mode.

and a time-dependent crack growth term:

$$\left[\frac{da}{dN}\right]_{total} = \left[\frac{da}{dN}\right]_{cyclic} + \left[\frac{da}{dN}\right]_{time\text{-}dependent} \quad (1)$$

Normally, the cyclic component is dependent upon the stress intensity range, ΔK and stress ratio, R. The time-dependent part is considered to be an integration over a cycle of the sustained load contribution to the crack growth,

$$\left[\frac{da}{dN}\right]_{time\text{-}dependent} = \int_{cycle} \frac{da}{dt}\,dt \quad (2)$$

Within the framework of these basic concepts, Nicholas [9] and Parida and Nicholas [10] incorporated additional factors in the form of coefficients in order to account for environmentally enhanced crack growth as well as the retardation effect due to crack-tip blunting. The equation, which considers the total cycle time, T, to affect the environmental degradation, and also incorporates the contributions of hold times (T_H) to blunting, has the form:

$$\left[\frac{da}{dN}\right]_{total} = F_1(T_H)\left[\frac{da}{dN}\right]_{cyclic} + F_2(T_H)T^{\gamma-1}\left[\int_{cycle}\frac{da}{dt}\,dt + T_H\frac{da}{dt}\right] \quad (3)$$

$$F_1(T_H) = (1+\mu T_H)^{-\alpha} \quad (4)$$

$$F_2(T_H) = 1+\beta(1+\mu T_H)^{-\alpha} \quad (5)$$

where T represents the total cycle time, α, β, γ, μ are parameters whose values need to be assigned for a given material to account for the experimentally observed fatigue crack growth behavior, and $F_1(T_H)$ and $F_2(T_H)$ are blunting coefficients which depend on hold time duration. Eq. (4) is of the form that as hold time increases, the cyclic growth rate is decreased because of blunting or stress relaxation at the crack tip. Eq. (5) has a form such that da/dt, which would occur under constant load (very long hold time), has a coefficient of one for very long hold times but the coefficient is greater than one for short or no hold times because the crack is sharper, or less blunt, than under sustained load without cycling. In the numerical computations, T_H is only considered when it occurs at maximum load. For holds at minimum load, T_H is taken as zero since it does not contribute to blunting, however total cycle time includes the hold time at either minimum or maximum load to account for the environmental effects. The magnitude of the time dependent term, da/dt, may be deduced for a given material from "creep-fatigue" tests involving cycles and hold times, as described by Saxena *et al.* [17],

$$\left[\frac{da}{dt}\right]_{avg} = \frac{1}{T_H}\left[(da/dN) - (da/dN)_0\right] \quad (6)$$

where da/dN is the FCGR at a given ΔK for a cycle with a superimposed hold time of T_H at P_{max} and $(da/dN)_0$ is the corresponding cyclic crack growth rate for zero hold time. Although this method seems to have worked reasonably well for nickel-base superalloys such as Inconel 718 and Rene 95 as well as for Cr-Mo-V steel, it is rather difficult to use for Ti-1100, since FCGR for hold time at P_{max} and that for zero hold time are almost identical as seen from Fig. 5. Since the value of da/dt in Eq. (3) corresponds to the contribution when hold times are zero, that is, immediately after fatigue cycling, this quantity cannot be readily obtained experimentally. Therefore, for the purpose of modeling in Eq. (3), a very small value of 2×10^{-9} m/s was chosen for the term da/dt to best fit the experimental data at $\Delta K = 20$ MPa$\sqrt{m}$ with this model. Similarly, $[da/dN]_{cyclic}$ has

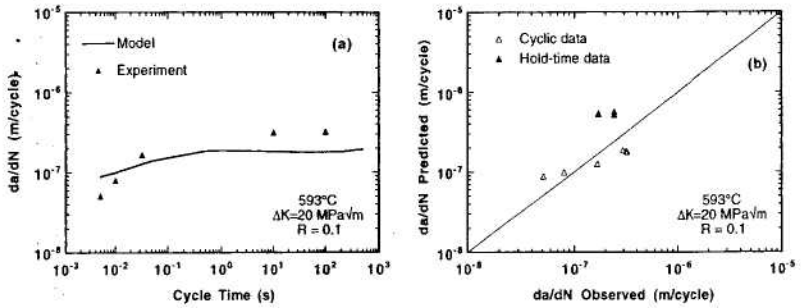

Fig. 10. Comparison of fatigue crack growth data with model predictions: (a) under pure cyclic loading. (b) including superimposed hold time.

to be chosen to represent the growth rate at frequencies higher than those used in the experiments, and corresponds to "purely cyclic" behavior. For a best fit of the data, a value of 7×10^{-8} m/cycle was chosen. The values for all of the parameters were obtained with the aid of a mathematical minimization routine combined with constraints on the parameters to make them physically meaningful. Through this process, numerical values of the other parameters obtained from the spread sheet are as follows: $\alpha = 0.75$, $\beta = 2000$, $\gamma = 0.7$, $\mu = 12$, when da/dN is expressed in m/cycle.

Figure 10(a) shows the model prediction and observed fatigue crack growth rate for the case of pure cyclic loading at 593°C and $R = 0.1$, corresponding to $\Delta K = 20$ MPa$\sqrt{m}$. The constants were obtained considering all of the data including the hold times at minimum and maximum loads. A better fit could be obtained for the cyclic data in Fig. 10, but the match of the hold time data would be worse. Nonetheless, the model captures the general features of the data which show an increase in growth rate at short cycle times and a leveling off of growth rate at higher cycle times.

Figure 10(b) shows predicted and experimental values of da/dN for all conditions including those of superimposed hold times at P_{max} and P_{min} over 1 Hz baseline cyclic loading. Note that the predicted results for pure cyclic loading agree reasonably well with experimentally observed values of fatigue crack growth rates. However, the growth rates predicted for superimposed hold times appear to be higher than the experimentally obtained values. This is attributed primarily to the peculiar alloy chemistry of this material which contributes to reducing the growth rate due to environmental effects with superimposed hold times, through an increased level of asperity-induced crack closure, associated with a change in mechanism of fracture as explained earlier. This produces a net increase in growth rate in air versus that in vacuum which is less than what might occur if the closure were not present. It appears that despite the difficulties encountered in predicting the crack growth rates for superimposed hold times, it is possible to represent its high temperature fatigue crack growth rate satisfactorily for pure cyclic loading by use of the above Superposition model which accounts for crack tip blunting as well as environmental effects. Better modeling of the environmental effects of this material would require a method to account for reduction of the effective stress intensity due to environmentally enhanced crack closure due to roughness.

CONCLUSIONS

1. Fatigue crack growth behavior of near-α titanium alloy Ti-1100 was studied under a wide range of loading frequencies and hold times at elevated temperature (593°C).

2. Fatigue crack growth resistance in this material is strongly influenced by the environment at 593°C. This is evident from the variation of FCGR with cycle time for pure cyclic loading, primarily at high frequency or short cycle time.

3. The rate of fatigue crack growth per cycle increases with decrease in cyclic loading frequency up to about $f=1.0$ Hz. On a da/dt basis, growth rate decreases continuously with increase in cycle time.

4. In the lower frequency range ($f=0.01$–1.0 Hz), the environmental effects appear to be counter-balanced by increased closure levels due to extensive crack branching and fracture surface asperities.

5. At $f \leqslant 1.0$ Hz the fatigue crack growth rate undergoes a transition at $\Delta K \approx 20$–25 MPa$\sqrt{m}$, when fracture mode changes from quasi-cleavage to ductile tearing with clear evidence of striated crack growth at higher SIF-range.

6. In the high frequency range ($f \geqslant 100$ Hz), crack growth rate levels off due to an absence of environmental effects and approaches that under a vacuum loading condition.

7. It is possible to use a simple superposition model to explain the observed fatigue crack growth behavior of this material under pure cyclic loading at 593°C. However, superimposed hold times over a baseline $f=1.0$ Hz cycle at maximum and minimum loads produce hardly any change in FCGR. This is indicative of the low sensitivity of this material to creep and environmental degradation at low frequencies and/or long cycle times.

8. Although fatigue crack growth rates at elevated temperatures are higher than those at room temperature, there is hardly any noticeable increase in growth rate between 593°C and 649°C at a frequency of 100 Hz and $R=0.1$ over most of the stress intensity range.

Acknowledgments—The support of the U.S. Air Force at the Wright Laboratory Materials Directorate, where this work was performed, is gratefully acknowledged. One of the authors (B.K.P.) would also like to thank the National Research Council for support through the Senior Resident Research Associateship program and the U.S. Air Force for support under the EOARD London Office "Window on Science" program.

REFERENCES

1. P. J. Bania (1988) An advanced alloy for elevated temperatures. *J. Metals* **40**(3), 20–22.
2. P. J. Bania (1988) *Ti-1100: A new elevated temperature titanium alloy*. Presented at the Sixth Int. Titanium Conference, Cannes, France.
3. H. Ghonem and R. Foerch (1990) Frequency effects on fatigue crack growth behavior in a near-a titanium alloy. In: *Elevated Temperature Crack Growth, MD-Vol. 18* (Edited by S. Mall and T. Nicholas). ASME, New York, pp. 93–105.
4. P. E. Irving and C. J. Beevers (1974) Microstructural influences on fatigue crack growth in Ti-6Al-4V. *Mater. Sci. Engng.* **14**, 229–238.
5. C. C. Chen and J. E. Coyne (1988) Relationships between microstructure and properties of Ti-6242-Si Alloy Forging. In: *Titanium 80: Science and Technology* (Edited by Camera and Zuni). p. 1197–1207.
6. J. A. Ruppen, C. L. Hoffman, V. M. Radhakrishnan and A. J. McEvily (1983) The effect of environment and temperature on the fatigue behavior of titanium alloys. In: *Fatigue, Environment and Temperature Effects, 27th Sagamore Army Materials Research Conference* (Edited by J. J. Burke and V. Weiss). Plenum Press, New York, pp. 265–300.
7. B. K. Parida and T. Nicholas (1993) effects of frequency and hold time on fatigue crack growth of Ti-1100 at high temperature. In: *FATIGUE 93*, (Edited by J. P. Bailon and J. I. Dickson). EMAS, Vol. II, pp. 859–864.
8. R. Foerch, A. Madsen and H. Ghonem (1993) Environmental interactions in high temperature fatigue crack growth of Ti-1100. *Metall. Trans.* (in press).
9. T. Nicholas (1991) Fatigue crack growth modeling at elevated temperature using fracture mechanics. In: *Elevated Temperature Crack Growth* (Edited by S. Mall and T. Nicholas). ASME. MD-Vol. 18, pp. 107–112.
10. B. K. Parida and T. Nicholas (1992) Frequency and hold time effects on crack growth of Ti-24 Al-11 Nb at high Temperature. *Mater. Sci. Engng* **A153**, 493–498.

11. H. H. Johnson (1965) Calibrating the electric potential method for studying slow crack growth. *Mater. Res. Standards* **5**, 442–445.
12. J. M. Larsen and T. Nicholas (1985) Cumulative damage modeling of fatigue crack growth in turbine engine materials. *Engng Fract. Mech.* **22**, 713–730.
13. T. Nicholas and S. Mall (1992) Elevated temperature crack growth in aircraft engine materials. In: *Advances in Fatigue Lifetime Predictive Techniques, ASTM STP 1122* (Edited by M. R. Mitchell and R. W. Landgraf). American Society for Testing and Materials, Philadelphia, 143–157.
14. N. Walker and C. J. Beevers (1979) A fatigue crack closure mechanism in titanium. *Fatigue Engng. Mater. Struct.* **1**, 135–148.
15. M. D. Halliday and C. J. Beevers (1981) Some aspects of fatigue crack closure in two contrasting titanium alloys. *J. Test. Eval.* **9**, 195–201.
16. R. H. Van Stone (1990) Comparison of interpolation and superposition models to predict time-dependent crack growth in Rene 95. In: *Elevated Temperature Crack Growth*, (Edited by S. Mall and T. Nicholas). MD-Vol. 18, ASME, New York, pp. 53–68.
17. A. Saxena, R. S. Williams and T. T. Shih (1981) A model for representing and predicting the influence of hold time on fatigue crack growth behavior at elevated temperature. In: *Fracture Mechanics, ASTM STP 743* (Edited by R. Roberts). American Society for Testing and Materials, Philadelphia, pp. 86–99.